Liver Cancer

Research Article

Liver Cancer
DOI: 10.1159/000531176

Received: January 5, 2023
Accepted: May 18, 2023
Published online: May 23, 2023

Multimodal Integrative Genomics and Pathology Analyses in Neoadjuvant Nivolumab Treatment for Intermediate and Locally Advanced Hepatocellular Carcinoma

Tan-To Cheung[a, b] Daniel Wai-Hung Ho[b, c] Shirley Xueying Lyu[b, c] Qingyang Zhang[b, c] Yu-Man Tsui[b, c] Tiffany Ching-Yun Yu[b, c] Karen Man-Fong Sze[b, c] Joyce Man-Fong Lee[b, c] Vince Wing-hang Lau[d] Edward Yin-Lun Chu[d] Simon Hing-Yin Tsang[a] Wong-Hoi She[a] Roland Ching-Yu Leung[e] Thomas Chung-Cheung Yau[b, e] Irene Oi-Lin Ng[b, c]

[a]Department of Surgery, School of Clinical Medicine, The University of Hong Kong, Hong Kong, Hong Kong SAR; [b]State Key Laboratory of Liver Research, The University of Hong Kong, Hong Kong, Hong Kong SAR; [c]Department of Pathology, School of Clinical Medicine, The University of Hong Kong, Hong Kong, Hong Kong SAR; [d]Department of Diagnostic Radiology, Queen Mary Hospital, Hong Kong, Hong Kong SAR.; [e]Department of Medicine, School of Clinical Medicine, The University of Hong Kong, Hong Kong, Hong Kong SAR

Keywords
Anti-PD-1 · Preoperative nivolumab · Resection · Multiomics

Abstract

Introduction: Immunotherapy has resulted in pathologic responses in hepatocellular carcinoma (HCC), but the benefits and molecular mechanisms of neoadjuvant immune checkpoint blockade are largely unknown. ***Methods:*** In this study, we evaluated the efficacy and safety of preoperative nivolumab (anti-PD-1) in patients with intermediate and locally advanced HCC and determined the molecular markers for predicting treatment response. ***Results:*** Between July 2020 and November 2021, 20 treatment-naive HCC patients with intermediate and locally advanced tumors received preoperative nivolumab at 3 mg/kg for 3 cycles prior to surgical resection. Nineteen patients underwent surgical resection on trial. Seven (36.8%) of the 19 patients had major pathologic tumor necrosis (≥60%) in the post-nivolumab resection specimens, with 3 having almost complete (>90%) tumor necrosis. The tumor necrosis was hemorrhagic and often accompanied by increased or dense immune cell infiltrate at the border of the tumors. None of the patients developed major adverse reactions contradicting hepatectomy. RNA-sequencing analysis on both pre-nivolumab tumor biopsies and post-nivolumab resected specimens showed that, in cases with major pathologic necrosis, the proportion of CD8 T cells in the HCC tissues predominantly increased after treatment. Moreover, to investigate noninvasive biomarker for nivolumab response, we evaluated the copy number variation (CNV) using target-panel sequencing on plasma cell-free DNA of the patients and derived a CNV-based anti-PD-1 score. The score

Tan-To Cheung, Daniel Wai-Hung Ho and Shirley Xueying Lyu contributed equally to this work.

Correspondence to:
Tan-To Cheung, cheung68@hku.hk
Thomas C.-C. Yau, tyaucc@hku.hk
Irene Oi-Lin Ng, iolng@hku.hk

correlated with the extent of tumor necrosis and was validated in a Korean patient cohort with anti-PD-1 treatment. ***Conclusion:*** Neoadjuvant nivolumab demonstrated promising clinical activity in intermediate and locally advanced HCC patients. We also identified useful noninvasive biomarker predicting responsiveness.

Introduction

Hepatocellular carcinoma (HCC) is one of the commonest malignancies worldwide and is highly prevalent in Asia [1]. HCC is an aggressive cancer and often diagnosed at advanced stages and is hence not operable. For operable HCC, surgical resection and liver transplantation are regarded as the main curative treatments for HCC. However, the use and benefit of neoadjuvant treatment for HCC before surgery are unclear, and there is a need for study.

HCC is notoriously highly resistant to conventional chemotherapy. Antibodies that block the immune inhibitory pathway of programmed death 1 (PD-1) protein have provided a modest treatment advance in HCC patients. In CheckMate 040, the first trial of immune checkpoint blockade (ICB) in patients with previously treated advanced HCC, PD-1 inhibitor nivolumab unleashed antitumor immunity, resulting in tumor regression and improved survival [2]. Of the patients evaluated, the best response rate was about 20%, and adverse events were manageable. Nivolumab monotherapy was later tested against sorafenib in the first-line setting for patients with advanced HCC, and an objective response rate of 15.4% with a favorable safety profile was reported [3]. With the successful advent of ICB, the combo of atezolizumab (anti-PD-L1) and bevacizumab (anti-VEGF) has become the new standard of care and first-line drugs for advanced HCC in 2020 [4], while the TKIs, sorafenib and lenvatinib, are now alternative first-line drugs for advanced HCC. However, all these treatments are often given on a "one-size-fits-all" basis, and the survival benefits are limited. Although there have been a couple of studies investigating the systemic use of anti-PD-1 in advanced HCC [5, 6], there is a general lack of biomarkers in predicting ICB response [7, 8], and the evidence supporting neoadjuvant use of nivolumab is scarce.

To this end, we performed this study to evaluate the efficacy and safety of the use of nivolumab as a presurgical neoadjuvant therapy in a group of mostly (70%) hepatitis B virus (HBV)-positive patients with intermediate and locally advanced HCC. To find out the determinants of nivolumab response, we also examined the relationship between the pathological response and cellular and molecular profiles of patients' HCC tumors, as well as the effects of nivolumab on the tumor immune microenvironment. Moreover, we further made use of plasma cell-free DNA (cfDNA) to derive a noninvasive biomarker that could predict the response toward anti-PD-1 ICB and may be useful to guide its administration.

Materials and Methods

The Study

This was a single-arm, single-center study designed to assess the clinical benefit of neoadjuvant treatment with nivolumab in patients with untreated, intermediate, and locally advanced HCC. The study was approved by the Institutional Review Board of the University of Hong Kong/Hospital Authority Hong Kong West Cluster and was conducted in compliance with International Conference on Harmonization Good Clinical Practice. All patients provided written informed consent. The study was registered on the ClinicalTrials.gov (study identifier: NCT05471674) and HKU Clinical Trials Registry (study identifier: HKUCTR-2807).

Patients

Eligible patients were aged ≥18 years with HCC, had no prior therapy, and had tumors considered intermediate or locally advanced tumor status per the Hong Kong Liver Cancer (HKLC) staging classification [9], Child-Pugh class A, Eastern Cooperative Oncology Group (ECOG) performance status score of 0 or 1, and adequate organ function. Patients were screened for comorbid conditions, and the operation's fitness was assessed by experienced anesthesiologists. Patients were required to provide a pretreatment fresh tumor biopsy sample. Exclusion criteria included extrahepatic metastasis, ascites requiring intervention, coinfection with HBV and hepatitis C virus (HCV), an HBV DNA level exceeding 500 IU/mL, and significant autoimmune diseases.

Trial Design

Twenty patients were enrolled in a consecutive manner in this study from January 2020 to December 2021. The patients' demographic data are shown in Table 1A. Patients were treated with intravenous nivolumab at 3 mg/kg on day one of each two weekly cycle for three cycles, followed by curative resection approximately 6 weeks after the first dose (Fig. 1a). The primary endpoint was pathologic response and safety of nivolumab. Secondary endpoints included recurrence-free survival, overall survival, and surgical outcome parameters.

Tumors were assessed by computed tomography (CT) or magnetic resonance imaging at baseline. Imaging assessment was repeated prior to surgery to reassess for resectability if feasible. Adverse events were continuously monitored and graded per the National Cancer Institute Common Terminology Criteria for Adverse Events, version 4.03. Resection was performed according to institutional practice. All the patients were followed up for recurrence-free survival and overall survival. The patients received contrast CT scan 1 month after the surgery and

Table 1. Patients' demographic data (**A**) and pathologic data (**B**)

A – Patients' baseline data	Neoadjuvant HCC study, *n* = 20
Age	65.2 (44.1–79.7)
Sex (male:female)	16:4
Hepatitis B carrier, %	
No	6 (30)
Yes	14 (70)
Tumor stage per HKLC, %	
Locally advanced	18 (90)
Intermediate	2 (10)
Child-Pugh grade A	20 (100)
ECOG, %	
0	12 (60.0)
1	8 (40.0)
Imaging tumor size pre-neoadjuvant treatment	13 (5.3–19.0)
Imaging tumor size post-neoadjuvant treatment (*n* = 15)	13.3 (4.6–20.8)
B – Pathologic data	Neoadjuvant HCC study with tumor resection, *n* = 19
No. of tumor nodules	1 (1 – multiple)
Tumor size, cm	13.0 (5.2–16.0)
Resection margin involved	None
Shortest resection margin, cm	0.5 (0.1–1.7)
Liver background disease (pathologic), %	
Chronic hepatitis with bridging fibrosis	13 (68.4)
Cirrhosis	6 (31.6)
Tumor cellular differentiation, %	
Well differentiated	6 (31.6)
Moderately differentiated	13 (68.4)
Poorly differentiated	0 (0)
Microvascular invasion	7 (36.8)
Absent Present	12 (63.2)
TNM tumor staging (UICC 8), %	
IB	4 (21.1)
II	3 (15.8)
IIIA	8 (42.1)
IIIB	4 (21.1)
BCLC staging, %	
A	1 (5.3)
B	10 (52.6)
C	8 (42.1)

every 3 months afterward. Patients had follow-up at 1 month and every 3 months at the clinics. At each attendance to the clinic, patients were fully assessed by clinicians, and blood was taken for complete blood picture, liver and renal function tests, prothrombin level, and AFP level. Chest X-ray examination was performed every 3 months.

Fresh pretreatment liver needle biopsies of HCC tumors were taken by experienced radiologists under ultrasound guidance to ensure safety and success of biopsy taking. After nivolumab treatment, all patients received surgical resection, and fresh tissues were taken from the resected tumors immediately in the operation theaters. In addition, peripheral blood samples were taken before and during nivolumab treatment, after surgical resection, and at multiple time points upon follow-up.

Pathologic Analysis

Pre-nivolumab treatment liver biopsies and posttreatment resected tumor specimens were examined and sampled thoroughly for histological examination (by IOLN). Fresh tissues were taken and processed for subsequent dissociation of cells. The surgical specimens were staged according to the criteria of the American Joint Committee on Cancer (8th edition) for evaluating tumor

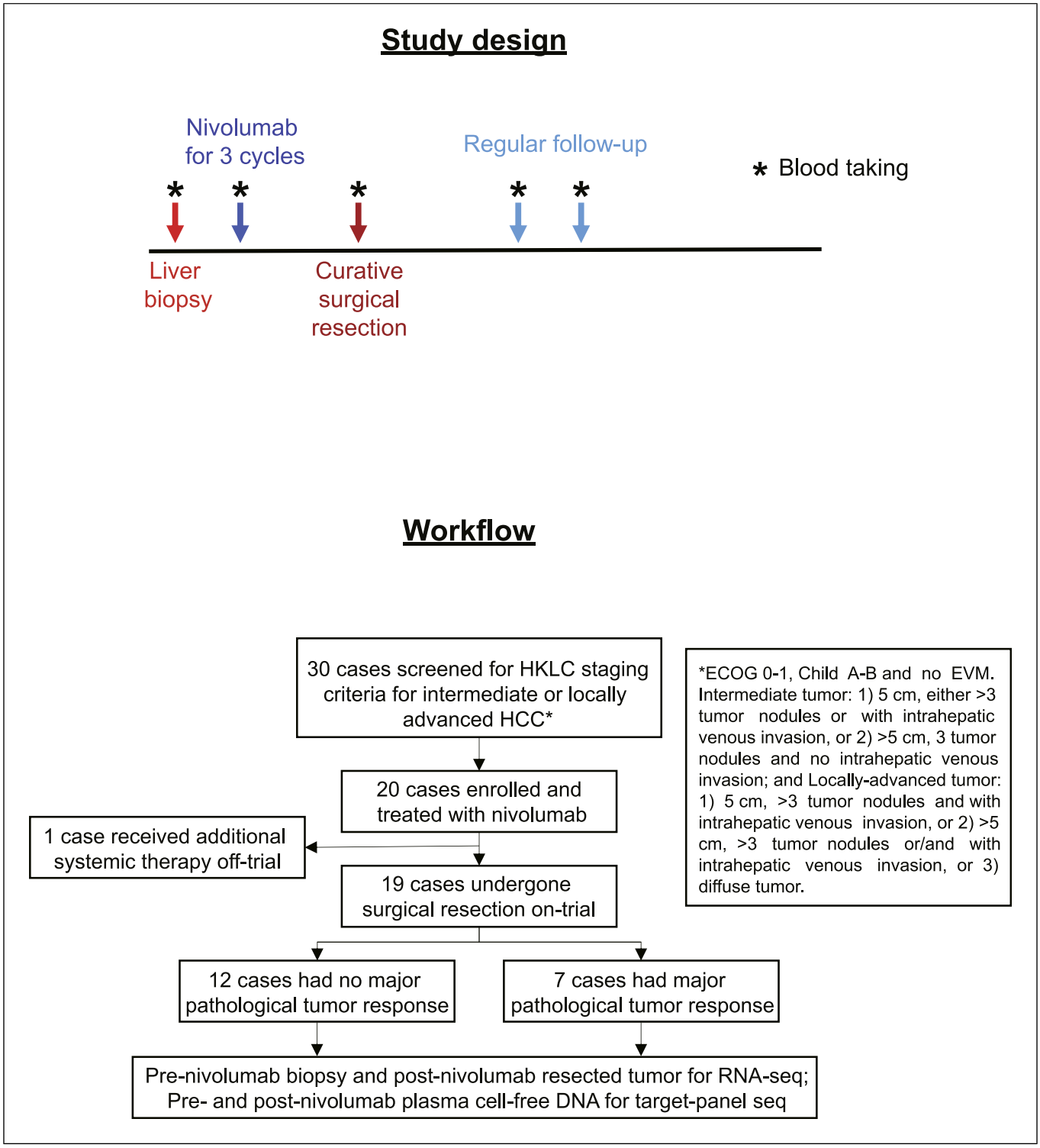

Fig. 1. Study design and workflow and patients' demographic data.

stage. Primary tumors were assessed for the percentage of necrosis by routine hematoxylin and eosin staining. A complete cross-sectional slab of the tumor was embedded in multiple blocks for formalin-fixed paraffin-embedded sections to ensure comprehensive sampling of the different areas of the tumor. All histological sections of the tumor slabs were assessed, and the

evaluation of the percentage of tumor necrosis by the pathologist was assisted by computational analysis using Nanozoomer Digital Pathology (by Hamamatsu Photonics K.K., Japan). On the digital slide, the total area of the tumor and the viable part were outlined by the pathologist. The total area of the tumor and the areas of the viable tumors were calculated by the software, and the percentage of tumor necrosis was then calculated by subtraction. The analysis of the T-cell numbers in the pretreatment biopsies and posttreatment resected specimens was based on immunohistochemical staining with anti-CD8 and anti-CD4 antibodies. Five high-power fields (HPFs) (×400 magnification) were counted using a 5-tier counting as follows: 0, <10/HPF; 1, 10–24/HPF; 2, 25–50/HPF; 3, 51–100/HPF; 4, >100/HPF.

DNA and RNA Extraction, Library Construction, Next-Generation Sequencing, and Data Preprocessing

Total RNA was isolated from the paired pre-nivolumab tumor biopsies and their corresponding resected tumor tissues, as previously described [10–12]. Similarly, plasma and peripheral blood mononuclear cells (PBMCs) were extracted from whole blood collected in EDTA tubes. Genomic DNA was extracted from the PBMC samples using our established method [13]. To extract cfDNA, 1.5–2 mL input of plasma was subjected to extraction using the cobas cfDNA Preparation Kit (Roche, 07247737190) according to manufacturer's instructions. The eluted cfDNA was subjected to quantitation by Qubit dsDNA HS Assay Kit (Thermo Fisher Scientific) and fragment analysis by the High-Sensitivity NGS Fragment Analysis Kit (Agilent, DNF474).

For transcriptome sequencing (RNA-seq), cDNA libraries were prepared by KAPA mRNA Hyper Prep Kit, with total RNA as starting material and following manufacturer's protocol. For target-panel sequencing (targeted-seq), DNA libraries were done using KAPA Hyper Prep Kit, with genomic DNA from PBMCs and cfDNA from plasma as input. The target panel for target-panel sequencing comprised 639 gene targets (online suppl. Table 1; for all online suppl. material, see https://doi.org/10.1159/000531176). Target capture was prepared based on the protocols of Roche SeqCap EZ HyperCap Workflow. Illumina NovaSeq 6000 was used for pair-end 151 bp sequencing. Library preparation and next-generation sequencing (NGS) were performed by Centre for PanorOmic Sciences of the University of Hong Kong. We subjected the RNA-seq and target-seq data to quality control filtering and adapter trimming (Trimmomatic; http://www.usadellab.org/cms/index.php?page=trimmomatic).

Bioinformatics Analyses

Transcriptome and target-panel sequencing reads were mapped to the reference human genome (hg38) using HISAT2 and Burrows-Wheeler Aligner, respectively. For the transcriptome sequencing data, raw read counts of genes were estimated by featureCounts [14] and tested for differential gene expression by DESeq2 [15]. Differentially expressed genes were defined as $p < 0.05$ and $|\log2(\text{fold change})| > 0.5$. Normalized read counts as transcripts per million were calculated [16]. Immune cell type abundance was inferred by cell deconvolution analysis using CIBERSORTx [17]. ToppGene suite [18] was used to perform gene set enrichment analysis for mechanistic evaluation on gene sets of Gene Ontology: biological process and Reactome pathway. Components of top gene sets were analyzed for protein-protein interaction using STRING database [19].

Regarding the target-panel sequencing data, PCR duplicate reads were removed, followed by indel realignment and base quality score recalibration. We applied filtering on sequencing reads based on fragment size to improve the sensitivity of our subsequent copy number variation (CNV) analysis. After calculating read depth for each exon region in the target panel, it was normalized based on the total read depth of each sample. To identify somatic CNV at gene intervals, we utilized CNVkit [20] to calculate the log2 ratio. We tested for variation on sequencing coverage on cfDNA, with the corresponding PBMC as a reference. We compared the log2 ratios of gene intervals between responsive and nonresponsive patients to confine the candidate CNV intervals that are associated with nivolumab response. Spearman's correlation between log2 ratio of gene intervals and patients' percentage of tumor necrosis was used to shortlist putative CNV intervals ($|\text{correlation}| > 0.4$ and $p < 0.05$) that harbor CNV associated with nivolumab response. Regarding somatic mutation identification, we utilized Lancet [21] and Mutect2 [22], with default parameters. Tumor mutation burden (TMB) was defined as the number of mutations per megabase (mut/Mb).

Circulating cfDNA, Genomic DNA, and CNV-Based Anti-PD-1 Response Score to Predict ICB Response

Blood samples were taken immediately prior to and upon completion of nivolumab treatment. cfDNA and genomic DNA were extracted from patients' plasma and PBMC, respectively. After subjecting them to target-panel sequencing, we applied necessary quality control and preprocessing on the read alignment. We enriched for cfDNA fragments likely to originate from malignant cells [23] by extracting shorter sequencing reads with fragment sizes <170 bp. Our fragment analysis result showed that cfDNA from HCC patients peaked at around 170 bp (online suppl. Fig. 1). With genomic DNA from the corresponding PBMC samples of the same individual patients, we determined the somatic copy number alterations at gene intervals.

To determine blood-based biomarker(s) that predicted anti-PD-1 ICB response in HCC patients, a drug response score was assessed by CNV intervals that were associated with the degree of tumor necrosis. We first shortlisted CNV intervals that possess statistically significant correlation between CNV status (in terms of log2 ratio) and the patients' degree of pathologic tumor necrosis (online suppl. Fig. 2). To avoid the domination by certain CNV intervals with extreme log2 ratios, we restricted the log2 ratios to be within −1 to 1, i.e., those log2 ratios above 1 were truncated as 1 and those below −1 as −1. We also discarded those CNV intervals having discordant correlation trends within the same gene. Next, we determined an anti-PD-1 response score that was a weighted average of the copy number status of those shortlisted CNV intervals and calculated by the summation of product between correlation coefficient and log2 ratio as follows:

$$\text{Anti-PD-1 response score} = \sum_{i=1}^{n} \rho(i)^{*} x(i)$$

where ρ and x were the Spearman's correlation coefficient with percentage of pathologic tumor necrosis and log2 ratio, respectively, of each CNV region. For validation of our discovery findings, we downloaded and compared the study data of a Korean group of HCC patients having undergone anti-PD-1 treatment

from Hong et al. [6]. In order to normalize the scales of the anti-PD-1 response score between datasets (our in-house and Hong et al. [6]), we performed additional standardization on the anti-PD-1 response score in each dataset:

$$\text{Standardized anti-PD-1 response score} = (\text{score} - \mu)/\sigma$$

where score was the anti-PD-1 score for a patient, and μ and σ were the mean and standard deviation of anti-PD-1 response scores, respectively, for the corresponding sample cohort.

Detection of HBV Integration

We had developed a fast and memory-efficient detection tool of viral integration sites called Virus-Clip [24, 25], which can identify the exact positions of viral integrations and automatically annotate the integration events with the corresponding affected human genes. We used Virus-Clip to identify HBV integration in the HBV-associated samples.

Statistical Analyses

The study was neither designed nor powered to test any statistical hypothesis. Safety data were summarized descriptively in the safety population, defined as all patients who had received nivolumab. Pathologic tumor response and other efficacy data were evaluated for patients in the safety population who had undergone curative resection. Recurrence-free survival was defined as the time from the date of surgery to the earlier of disease recurrence or death from any cause. Overall survival was defined as the time from the start of nivolumab treatment to the death from any cause. Time-to-event data were summarized by Kaplan-Meier method. Median duration of follow-up was summarized by reverse Kaplan-Meier method. Reported Fisher Exact *p* values were one-sided, and the significance level was set at 0.05 for all analyses unless otherwise stated.

Results

Clinical Findings

From July 2020 to November 2021, 30 patients were screened for eligibility. Twenty eligible patients were treated in the study. The patient characteristics at baseline are shown in Table 1A. The majority (90%) of patients had locally advanced stage, 10% had intermediate stage per Hong Kong Liver Cancer (HKLC) staging classification [9], and 2 patients had tumor thrombosis in the portal vein branch but without invasion to the main portal vein. The CT scan imaging tumor size ranged from 4.8 to 16.0 cm in the largest dimension, with a median of 13.0 cm. 70% ($n = 14$) of the patients were HBV carriers, and the remaining 5 were alcohol-associated HCC; none had HCV infection by serological anti-HCV antibody. Fifteen patients had preoperative medical conditions which had no absolute contraindication to surgery.

All 20 patients completed the planned neoadjuvant therapy regimen. One patient received additional systemic therapies off trial before surgery and was thus considered not having undergone surgery on trial in the efficacy analyses (Fig. 1b). None of the patients developed adverse reaction to nivolumab contradicting from receiving hepatectomy. Treatment-related adverse event occurred in only one (5%) of the 20 patients, which was grade 2 hypocortisolism developed prior to surgery and managed by corticosteroid replacement. Of those 19 patients having undergone surgery on trial, 15 (78.9%) received major liver resection and 4 (21.1%) received minor liver resection. The median operation time was 215 min. Three (21.1%) patients developed postoperative complications with Clavien complication >3a. The median hospital stay was 8 days, and there was no hospital mortality. The operation details are listed in Table 2.

Pathologic Tumor Necrosis after Nivolumab Treatment

The percentage of necrosis in the pretreatment needle-biopsied HCC tissues ranged from 0 to 70%, with a median of 5% and a mean of 16.4%. However, the percentage of necrosis detected in the pretreatment needle biopsies had limitation of sampling error and small size of the needle-biopsied tissues. The resected tumors ranged from 5.2 to 16 cm, with a median of 13 cm (Table 1B). Six patients (31.6%) had liver cirrhosis, and 13 patients (68.4%) had chronic hepatitis with bridging fibrosis without formation of regenerative nodules. Twelve (63.2%) patients demonstrated microvascular invasion histologically, and 12 (63.2%) patients had TNM staging IIIA and IIIB disease.

The tumor necrosis of the resected specimens ranged from 5% to 100% (Fig. 2a). Seven (36.8%) HCCs had significant (≥60%) tumor necrosis, and 3 of them had almost complete (>90%) tumor necrosis; 1 of these patients had complete pathologic response (100% necrosis in the tumor), notwithstanding that she had ruptured HCC after the second dose of nivolumab and was treated with transarterial embolization. In this study, those tumors with ≥60% tumor necrosis were considered "nivolumab-responsive" (nivo-R) and the others "nivolumab-nonresponsive" (nivo-NR) (Fig. 2). Hence, 7 and 12 patients were considered nivo-R and nivo-NR, respectively.

Outcome of Patients

The median follow-up was approximately 15 months (range: 2–25 months) (up to November 2022). Of the

Table 2. Operation details

Operation data	Received hepatectomy on trial, *n* = 19
Blood loss, L	1.5 (0.05–13.1)
Blood replacement, L	0.32 (0.0–5.19)
Blood transfusion [if yes, (%)]	10 (52.6%)
Total operation duration, min	215.0 (91–548)
Magnitude of liver resection	
Major resection	15 (78.9)
Minor resection	4 (21.1)
Multiple resection [yes (%)]	1 (5.3)
Type of resection	
Right hepatectomy	6 (31.6)
Right extended hepatectomy	3 (15.8)
Left extended hepatectomy	3 (15.8)
Left trisectionectomy	1 (5.3)
Segmentectomy	3 (15.8)
Subsegmentectomy	1 (5.3)
Central bisectionectomy	2 (10.5)
Complication data	**Neoadjuvant HCC study with tumor resection, *n* = 19**
Abdominal drain inserted [yes (%)]	13 (68.4)
Overall complication	4 (21.1)
Complications (could have ≥1)	
Pleural effusion tapping not required	1 (5.3%)
Pleural effusion tapping required	1 (5.3%)
Cardiac arrhythmia	1 (5.3%)
Bile duct obstruction	1 (5.3%)
Subphrenic collection	3 (15.8%)
Postop complication(s) – Clavien 3a or above	3 (15.8%)
Hospital stay, days	8.0 (3–45)
Hospital mortality	0 (0.0%)

7 nivo-R patients, all were alive as of November 2022, and 3 of them (42.9%) experienced tumor recurrence. For the 12 nivo-NR patients, 2 (16.7%) had died and 7 (58.3%) had tumor recurrence (Fig. 2a). Of these 2 patients who had died, 1 patient (57 years old) died of recurrent disease, whereas the other 80-year-old patient without tumor recurrence died of toxic epidermal necrolysis >3 months after surgery (most likely related to the prolonged use of antibiotics for treatment of postoperative collections). The 1-year overall survival was 89.5% (nivo-R group: 100%; nivo-NR group: 83.3%; slightly higher in the nivo-R group), and the overall 1-year tumor recurrence rate was 36.8% (nivo-R group: 28.6%; nivo-NR group: 41.7%; slightly lower in the nivo-R group) (Fig. 2b). Regarding the 3 nivo-R patients with >90% tumor necrosis, they were all alive and recurrence-free at the latest follow-up, indicating that a high degree of tumor necrosis after neoadjuvant nivolumab treatment might indicate durable response.

A total of 9 patients had increased serum alpha-fetoprotein (AFP) levels of >20 ng/mL at baseline before nivolumab, but the baseline AFP levels were not particularly associated with nivolumab response. All nivo-R patients showed some degree of reduction in the AFP level in the course of nivolumab treatment, although not reaching statistical significance ($p = 0.068$) (Fig. 2c). There was a trend that some of the nivo-R patients experienced a decline in AFP level. On the other hand, 5 of nivo-NR patients experienced an increase in AFP level after 3 cycles of nivolumab treatment but before surgical resection.

Pathology and CT Imaging

Pathologic analysis of the completely resected liver tumors showed various degrees of tumor necrosis as early as after 3 doses of nivolumab administration. Of note, the tumor necrosis was often hemorrhagic necrosis (Fig. 3a), which is not commonly seen in untreated HCC tumors

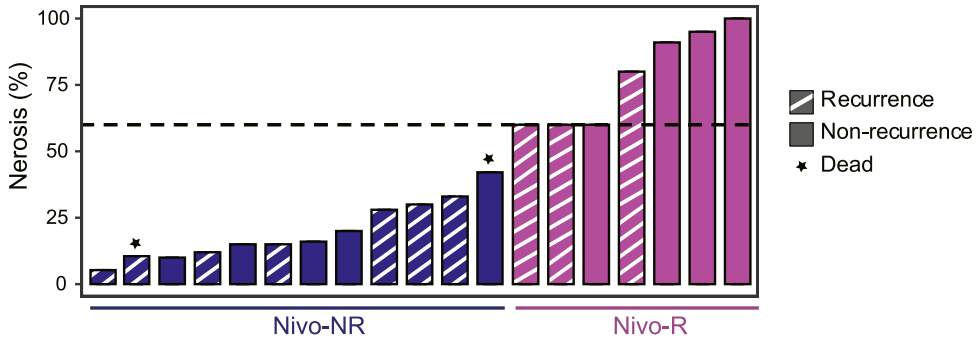

a

Patients'outcome

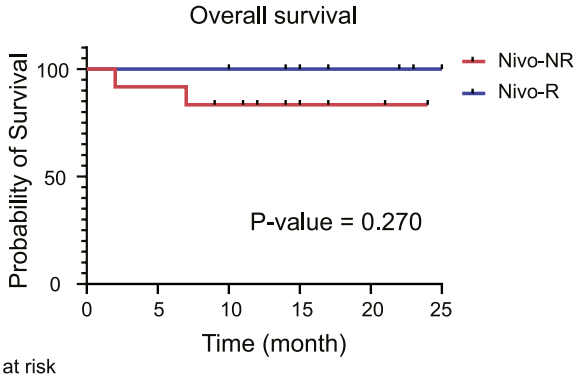

at risk

Nivo-NR	12	11	9	5	3	0
Nivo-R	7	7	7	5	3	1

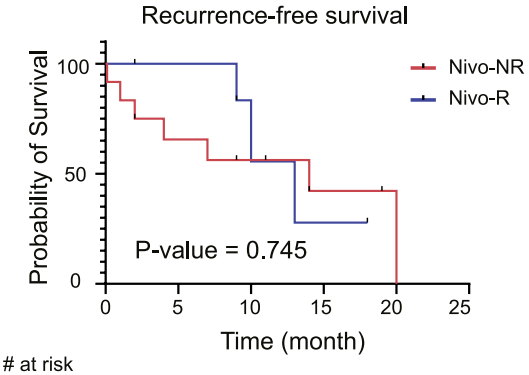

at risk

Nivo-NR	12	7	5	2	1	0
Nivo-R	7	6	3	1	0	0

b

1-year overall survival	
Nivo-R	100%
Nivo-NR	83.3%

1-year recurrence rate	
Nivo-R	28.6%
Nivo-NR	41.7%

Changes in AFP level at different time-points

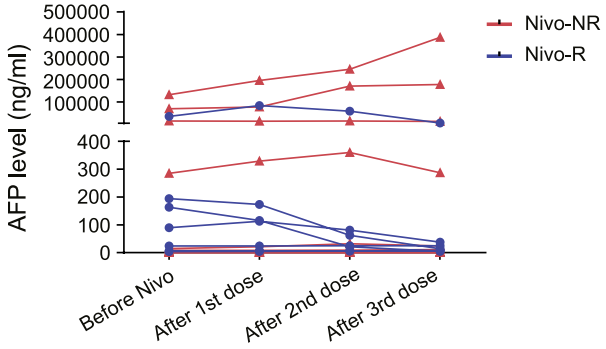

c

AFP level increase		
	Yes	No
Nivo-R	0	7
Nivo-NR	5	7
Fisher's P	0.068	

2

(For legend see next page.)

and was seen in both gross examination and histology. The tumor necrosis was often accompanied by increased or even dense immune cell infiltrate (mainly T cells), particularly at the border of the tumors.

As the percentages of tumor necrosis were assessed in the resected tumors, they should more accurately reflect the true extent of tumor necrosis than imaging assessment. A decrease in the percentage change of image size was seen in some of the tumors with major pathologic tumor necrosis (Fig. 3b, left panel), and there was mild but significant correlation between the percentage change of CT image size and pathologic tumor necrosis (Spearman $r = -0.559$, $p < 0.05$, Fig. 3b, right panel).

Whole-Transcriptome Sequencing (RNA-Seq) on Patient-Derived Tissue and Blood Samples

We performed RNA-seq on both pre- and post-nivolumab tumor tissues and PBMC samples in all 19 cases. The tissue and PBMC samples were largely and widely separated from one other, indicating their expected major intrinsic differences in gene expression (online suppl. Fig. 3). Moreover, the relatively higher degree of variability among the tissue samples, as compared to those of their PBMC counterparts (online suppl. Fig. 3), implies that the molecular differences in gene expression in tissue samples would serve as better biomarkers reflecting the underlying clinical diversity among the cases.

Changes in the Cellular Landscape of the Tumor Immune Microenvironment in Response to Nivolumab

We utilized cellular deconvolution algorithm [26, 27] to evaluate the cellular landscape of the tumor microenvironment and the immunological compositions of samples. By comparing the temporal transition of the cellular composition before and after nivolumab treatment, we observed disparate changes in certain immune cell types that contrasted between the nivo-R and nivo-NR cases. Notably, in those cases with major pathologic response (≥60% tumor necrosis), the proportion of CD8 T cells tended to increase after treatment, whereas those of CD4 memory resting T cells and resting mast cells declined (all Fisher's exact $p > 0.05$) (Fig. 4a). The changes in the T cells were in line with the mode of action of nivolumab, which mainly targets the PD-1 on the surface of T cells (CD8 T cells in particular). Nevertheless, the increase in the CD8 T-cell proportion may indicate the patients with significant pathologic response had better restoration in cytotoxic T-cell infiltration into the tumor, which is crucial in eliciting an effective antitumor action (Fig. 4b). Immunohistochemistry (IHC) confirmed the changes in the proportions of CD8 and CD4 T cells in patients' paired biopsies and resected tumor tissues to be substantially consistent with the cellular deconvolution results (both Kappa $p < 0.01$). Consistent with the findings using immune deconvolution, the IHC data showed an increase in CD8 T cells (Fisher's exact $p < 0.05$) and a trend of decrease in CD4 T cells (Fisher's exact $p > 0.05$) in the nivo-R cases as compared to the nivo-NR counterparts, implicating their functional roles in governing nivolumab response.

Changes in Immune Checkpoint Landscape after Nivolumab Treatment

We observed a general elevation in the expression of PD-1-related molecules after nivolumab treatment, and this was particularly prominent in the nivo-R cases (Fig. 5a). This suggests that the nivo-R cases might be more addicted to or had higher reliance on PD-1 immune checkpoint as their means of tumor escape. On the other hand, upon nivolumab treatment, there was a significant increase in the expression of the co-inhibitory checkpoint molecule CTLA4 in the nivo-R cases, suggesting a potential alternative immune escape mechanism elicited by more responsive HCC tumors after nivolumab treatment (Fig. 5b, upper panels). In addition, specific to the nivo-R cases, we observed a general upregulation of other co-inhibitory checkpoint molecules, e.g., HAVCR2, LAIR1, and TIGIT, suggesting potential additional layers of bypass mechanism upon ICB. Moreover, there was significant upregulation of several co-stimulatory checkpoints specific to the nivo-R cases but not in the nivo-NR cases, suggesting that the status of co-stimulatory checkpoint components may also be important in determining the ultimate nivolumab response (Fig. 5b, lower panels).

Fig. 2. Patients' treatment response. **a** The percentages of pathologic tumor necrosis in the resected hepatectomy specimens and follow-up of patients regarding disease recurrence. **b** Overall and recurrence-free survival of the patients. The 1-year overall survival rate was higher and the 1-year tumor recurrence rate, respectively, was lower in the nivo-R group than the nivo-NR group. **c** The changes in serum AFP levels at different time points are shown. All nivo-R patients showed no increase in AFP level in the course of nivolumab treatment, although not reaching statistical significance.

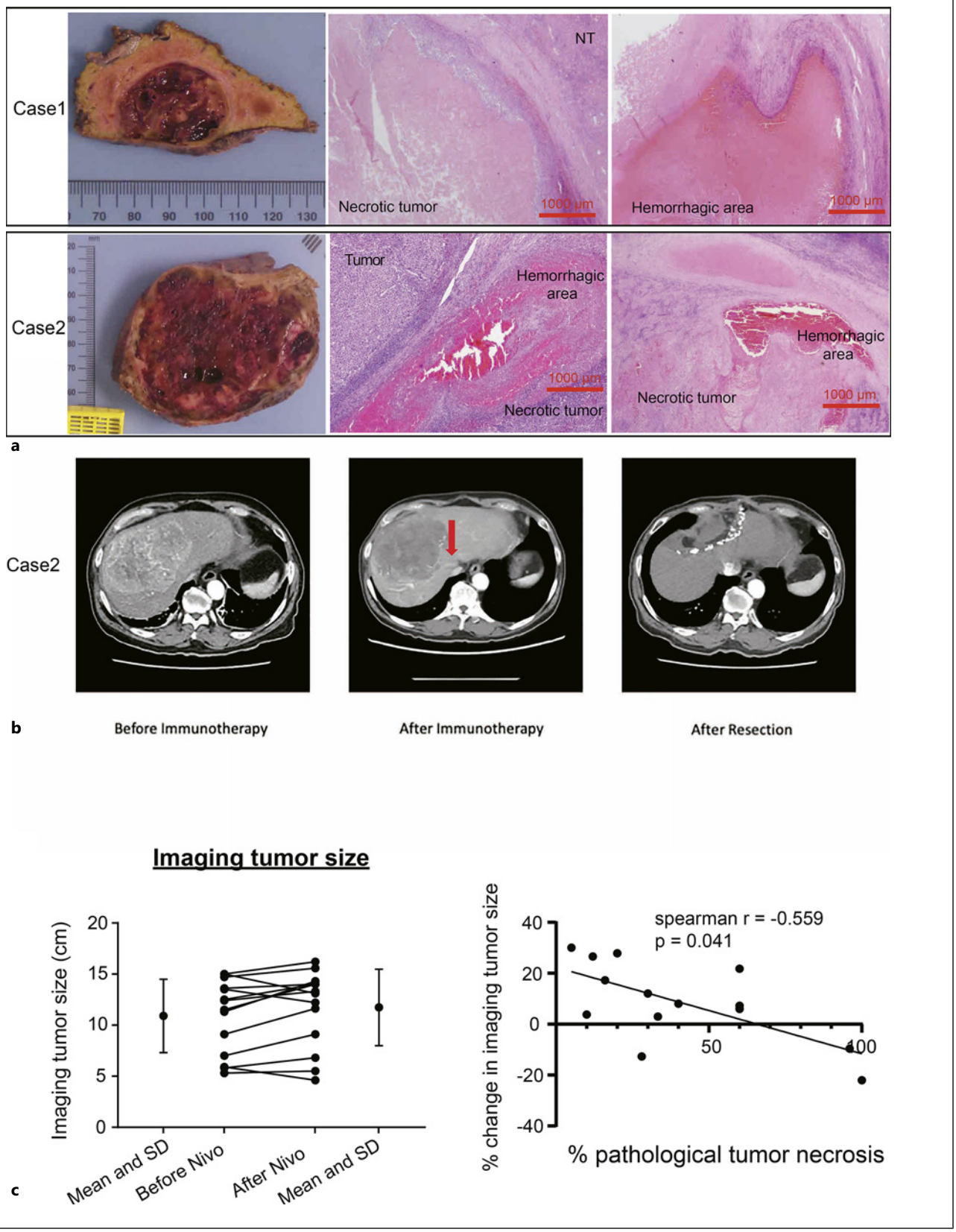

3

(For legend see next page.)

Mechanistic Investigation Revealed Immune-Related Pathways Advising Nivolumab Responsiveness

To evaluate the mechanistic overview of ICB, we compared the transcriptomic profiles of nivo-R and nivo-NR cases before and after nivolumab treatment and subjected them (upregulated genes: 2,691; downregulated genes: 1,640) to gene set enrichment analysis. Regarding the samples after nivolumab treatment, consistent with our findings in the cellular landscape, we detected an overall upregulation of immune response, particularly lymphocyte activation and differentiation (Fig. 6a). Besides, the differentially expressed genes could also differentiate the patients according to nivolumab response (online suppl. Fig. 4). Taken together, concordant insights from both cellular and molecular landscapes pinpointed the importance of T-cell activation and infiltration to elicit more effective ICB and hence their responsiveness in HCC patients. This signifies the potential of using T-cell-based biomarker to advise ICB outcome in advance.

More importantly, we aimed to delineate the underlying molecular determinants that advised the responsiveness toward nivolumab, particularly using the pre-nivolumab tumor biopsy samples. To address this, we compared the transcriptomic profiles of pre-nivolumab tumor biopsy samples between the nivo-R and nivo-NR cases to identify differentially expressed genes (upregulated genes: 304; downregulated genes: 1,255) related to different processes. We identified innate immunity-related functional enrichment to be the key factor related to nivolumab responsiveness (Fig. 6b). Of note, phagocytosis and complement activation were hallmarks identified in nivo-R patients, as compared to the nivo-NR counterparts. This may likely imply the intrinsic differences in the tumor microenvironment and, more importantly, the modulating role of innate immunity in governing ICB outcome.

Genomic Landscape and CNV-Based Biomarker Pinpointing Differential Nivolumab Treatment Outcome

The CNV-based anti-PD-1 response score we devised using target-panel sequencing on patients' plasma cfDNA significantly correlated with the extent of tumor necrosis in nivolumab-treated patients (Fig. 7a, left panel) and was able to stratify the patients according to their responsiveness toward nivolumab (Fig. 7a, right panel). To complement our CNV-based biomarker in predicting anti-PD-1 response, we obtained the whole-exome sequencing data from a Korean study with anti-PD-1 treatment on HCC patients by Hong and colleagues [6]. Using our derived algorithm, we similarly calculated the CNV-based anti-PD-1 response score using their data generated from tumor biopsy tissue samples. Consistent with our discovery findings derived from cfDNA, we could also differentiate nivo-R and nivo-NR patients according to the CNV-based anti-PD-1 response score on their patients (Fig. 7b). Importantly, by applying the anti-PD-1 response score on the combined sample cohort of ours and that of Hong et al. [6], we achieved an AUC value of 80.2% in distinguishing the treatment response of the patients (Fig. 7c).

On the other hand, the role of TMB in predicting response to ICB remains controversial [28, 29]. We identified somatic mutations in cfDNA extracted from the patients' pretreatment plasma samples. We calculated the TMB and compared it between the nivo-R and nivo-NR cases. It was found to be not statistically different based on our examination using the combined sample cohort (ours and that of Hong et al. [6]) (online suppl. Fig. 5). Moreover, we also determined the mutational landscape in our cohort and compared the profile between the nivo-R and nivo-NR cases (online suppl. Fig. 6). Regarding various key signaling pathways or processes, there were suggestive mutational differences related to anti-PD-1 response. Intriguingly, the suggestive trends regarding anti-PD-1 response were related to CDKN2A mutations (detected only in some nivo-NR cases and none in the nivo-R cases) and the enriched mutations detected in nivo-NR cases, including epithelial mesenchymal transition, p53, G2-M checkpoint, and PI3K/AKT/mTOR signaling pathways. Due to the previous investigations by others suggesting the association between CDKN2A alterations and reduced susceptibility to ICB [30, 31], we looked into CDKN2A

Fig. 3. a Representative cases showing gross pathology and histology of the resected specimens after preoperative nivolumab treatment. **b** Serial CT scan of the tumor change of a patient after neoadjuvant anti-PD-1 treatment (case 2 in **a**). A 12-cm tumor occupied the right lobe of the liver with compression of the middle and right hepatic veins. After nivolumab for 3 cycles, significant necrosis of the tumor was observed with the CT scan showing decreased vascular uptake and reduction in size of the liver lesion. The right hepatic vein (arrow) also became visible. A central hepatectomy was performed, and the CT scan done 4 months after liver resection showed no tumor recurrence. Clinically, he had no tumor recurrence 14 months after resection at the latest follow-up. **c** CT imaging tumor size of the 19 patients (left panel) and correlation between % change of CT imaging tumor size and % of pathologic tumor necrosis in the resected liver specimens (right panel).

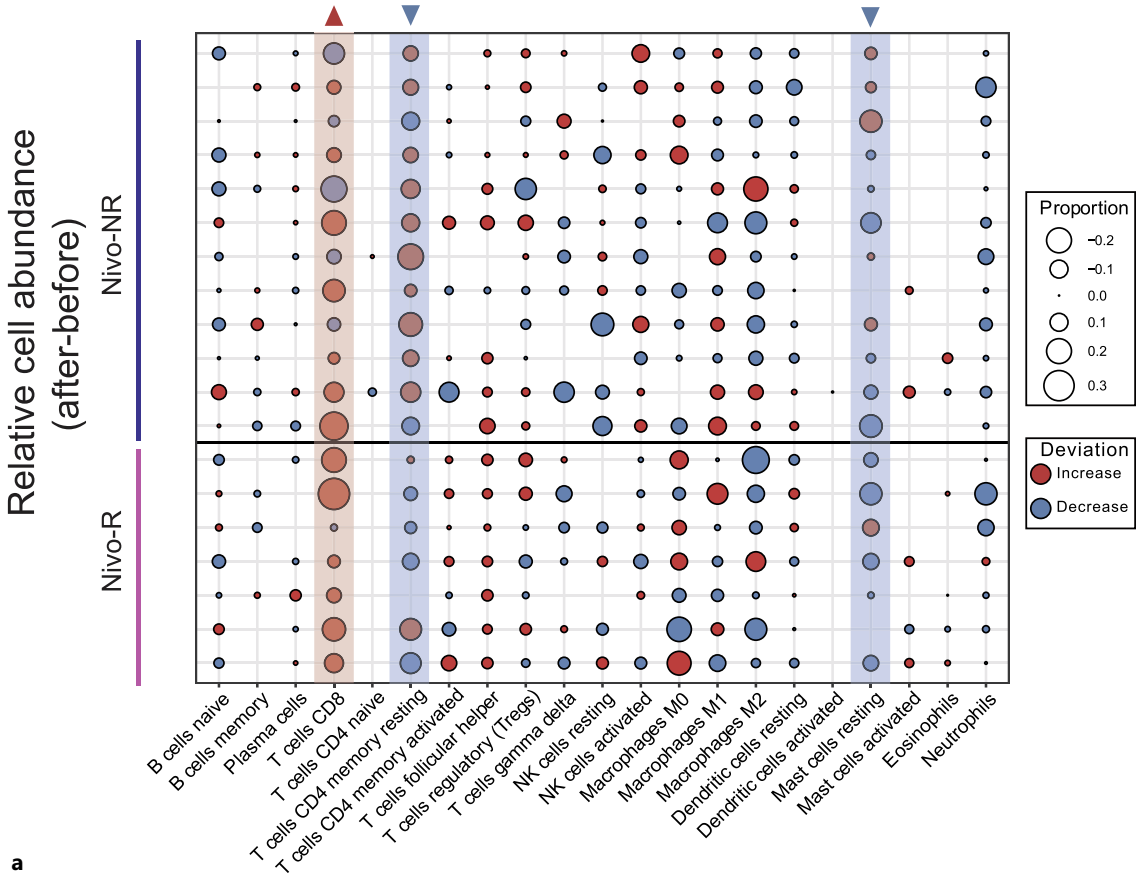

a

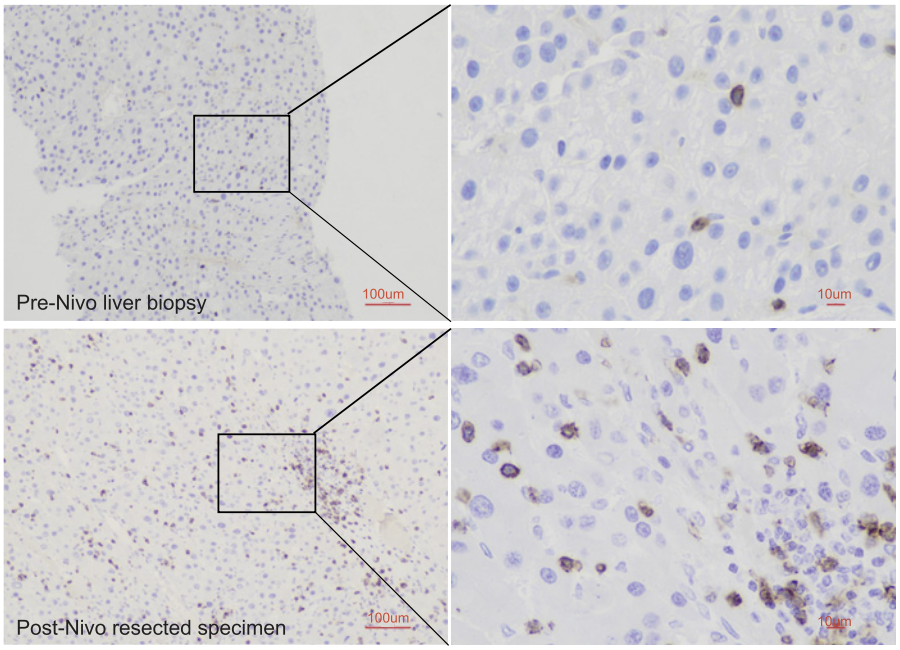

b

4

(For legend see next page.)

mutations using the combined sample cohort, but it had only near-to-random predictive power on anti-PD-1 response (online suppl. Fig. 7). Similarly, the mutations in the aforementioned signaling pathways were not predictive (online suppl. Fig. 7).

We also examined the HBV integration landscape in the cfDNA samples and were able to detect HBV integration in some (N = 8) cases, noting, however, that the sample size of detectable HBV-integrated cases was small. We detected no major differences between the nivo-R and nivo-NR cases (online suppl. Fig. 8). This may, to some extent, lend support that our findings regarding the exploration of nivolumab response using a cohort of largely HBV-positive cases may unlikely be restricted to HBV-associated HCCs.

Collectively, somatic mutations were less informative than CNV in determining anti-PD-1 response. Taking both somatic CNV and mutations into account, our findings suggest that HCC patients likely have intrinsic genomic differences, which govern their outcomes in ICB treatment.

Discussion

While there have been promising results of ICBs in the management of advanced HCC, the neoadjuvant use of anti-PD-1 treatment warrants a full investigation, preferably in patients with pathologic examinations. In our current study, the use of 3 doses of nivolumab nicely filled the treatment gap for patients from diagnosis to actual operation in a busy institute for HCC management. It has been reported that in patients with advanced HCC, the response rate to single and double immune checkpoint inhibitor (ICI) agents is around 20% and 32%, respectively [32, 33]. In this study, we demonstrated that neoadjuvant nivolumab ICB had a relatively high response rate of 36.8% in our predominantly HBV-positive HCC patients with intermediate and locally advanced tumors. Almost complete (>90%) tumor necrosis was seen in ~16% of the cases. Of note, this neoadjuvant nivolumab treatment was given for only 3 doses and within a relatively short period of time prior to surgery, implicating its potential efficacy in leading to tumor necrosis.

It is interesting to find that the post-nivolumab resection specimens showed conspicuous hemorrhagic necrosis both in the gross specimens and histology. Such hemorrhagic necrosis has not been reported even in a recent study by Simoes and colleagues, reporting for the first time the pathology in HCC resection specimens following nivolumab treatment [34]. On the other hand, tumor-infiltrating lymphocytes, present both within the tumors and around the tumor necrosis areas, likely represent the immune reaction elicited by anti-PD-1 action, as seen in that and our studies [34].

To date, despite some recent reports [35–37], there is still a scarcity of information about the neoadjuvant use of anti-PD-1 ICB. Among them, the phase 2 trials by Kaseb et al. [37] and Marron et al. [36] investigated the perioperative use of anti-PD-1 ICB, i.e., the ICB was also given after tumor resection. In this regard, this may preclude direct comparison with them on the neoadjuvant use of ICB. On the other hand, the study by Ho et al. [35] investigated the neoadjuvant use of cabozantinib plus nivolumab prior to surgical resection. With the primary aim of evaluating the possibility of converting locally advanced HCC into resectable disease, most (87.6%) of the enrolled patients went ahead with surgical resection irrespective of their status of pathologic response. In fact, of the 12 resected patients, 5 (42%) had major pathologic response (defined by ≥90% tumor necrosis), whereas the remaining ones did not have such major pathologic response. Another point of note is that they used double agents for treatment, and the treatment-related adverse events were quite frequent (in 93.3% of the cases), with 13.3% having grade 3 or above. Transient dose interruptions of cabozantinib were needed in 40% of the cases, and 13% even required dose reduction. In contrast, single-agent nivolumab was used in our study, and the treatment-related adverse event occurred in only 1 of the 20 patients treated, and it was grade 2 hypocortisolism manageable by corticosteroid replacement. Given the similar dosage of nivolumab used (our study: 3 mg/kg and Ho et al.: 240 mg; both intravenously), the major difference in treatment-related toxicity may likely hinge upon the double agents used in their study.

Our findings also provided useful insight into explaining the underlying differences in nivolumab treatment response. We found disparate changes in certain immune

Fig. 4. Dynamics of cellular landscape in related to nivolumab treatment. **a** Changes in the proportions of major immune cell types upon nivolumab treatment. **b** Immunohistochemical staining of CD8 in the resected specimen of a representative NR patient before (in liver biopsy) and after nivolumab treatment (in resected hepatectomy specimen). Nivo-R, nivolumab responsive; nivo-NR, nivolumab nonresponsive.

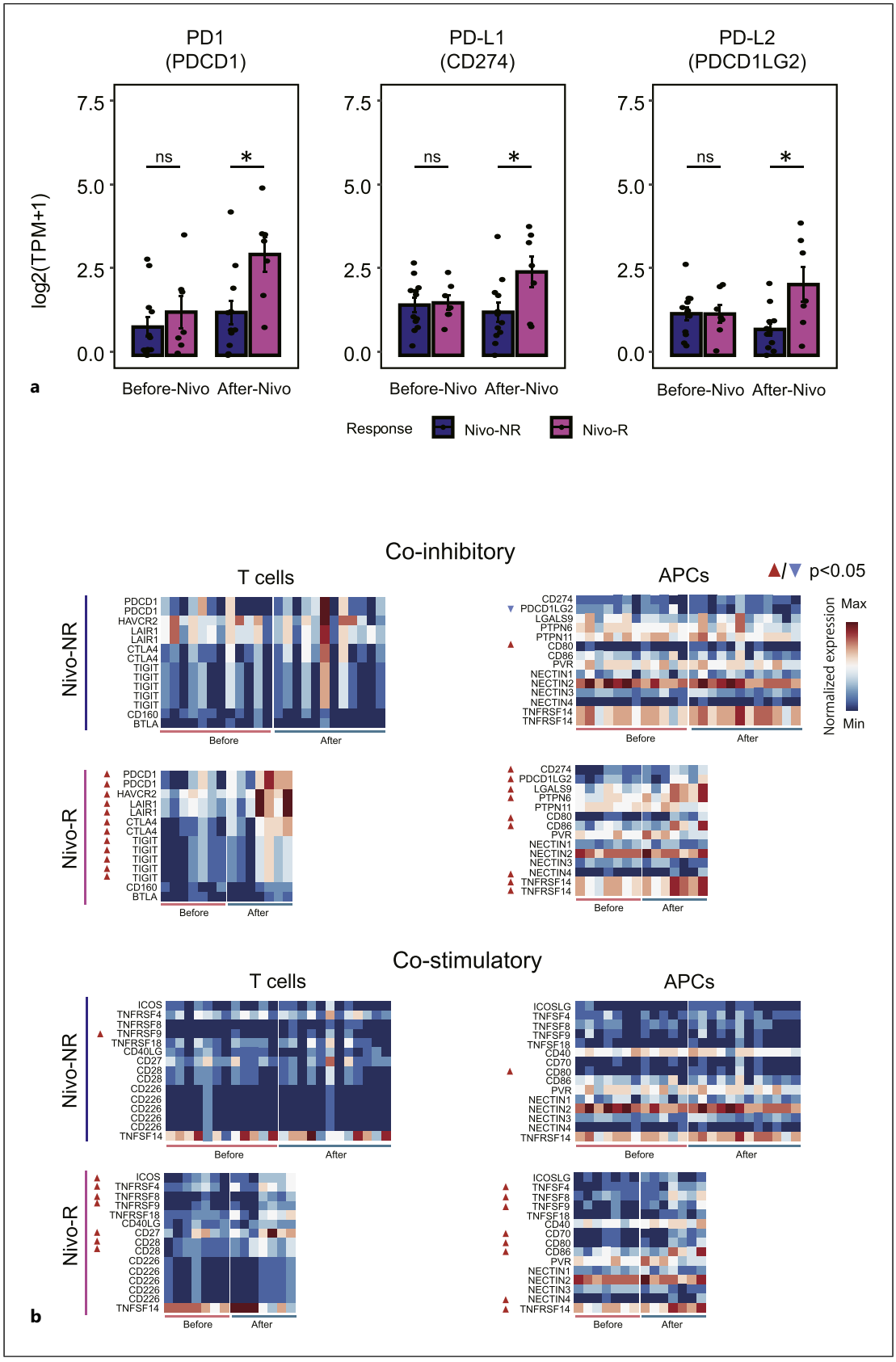

Fig. 5. Dynamics of immune checkpoint and transcriptomic landscapes in related to nivolumab treatment. **a** Gene expression changes in PD-1-related immune checkpoint components. **b** Gene expression changes in co-inhibitory (upper panel) and co-stimulatory (lower panel) immune checkpoint components. 2-sided Mann-Whitney U Test. * $p < 0.05$, ns: $p > 0.05$.

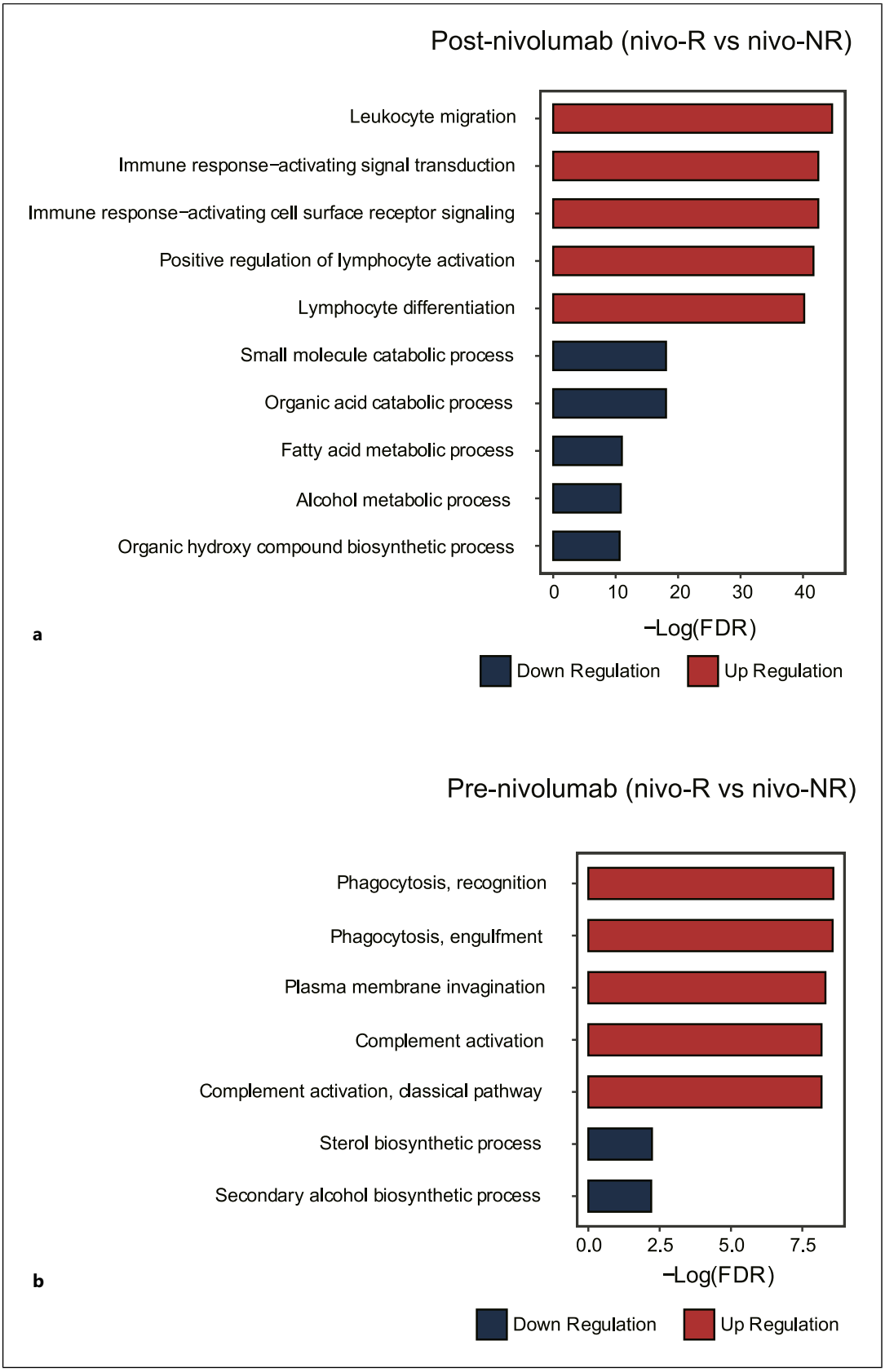

Fig. 6. Gene set enrichment analysis. Transcriptome analysis of post-nivolumab resected liver specimens (**a**) and the pre-nivolumab liver tumor biopsy samples (**b**) between the nivo-R and nivo-NR groups. Regarding post-nivolumab samples, we identified upregulation of immune-related processes, particularly lymphocyte activation and differentiation, in nivo-R cases, whereas innate immunity-related functional enrichment such as phagocytosis and complement activation was enriched in pre-nivolumab samples.

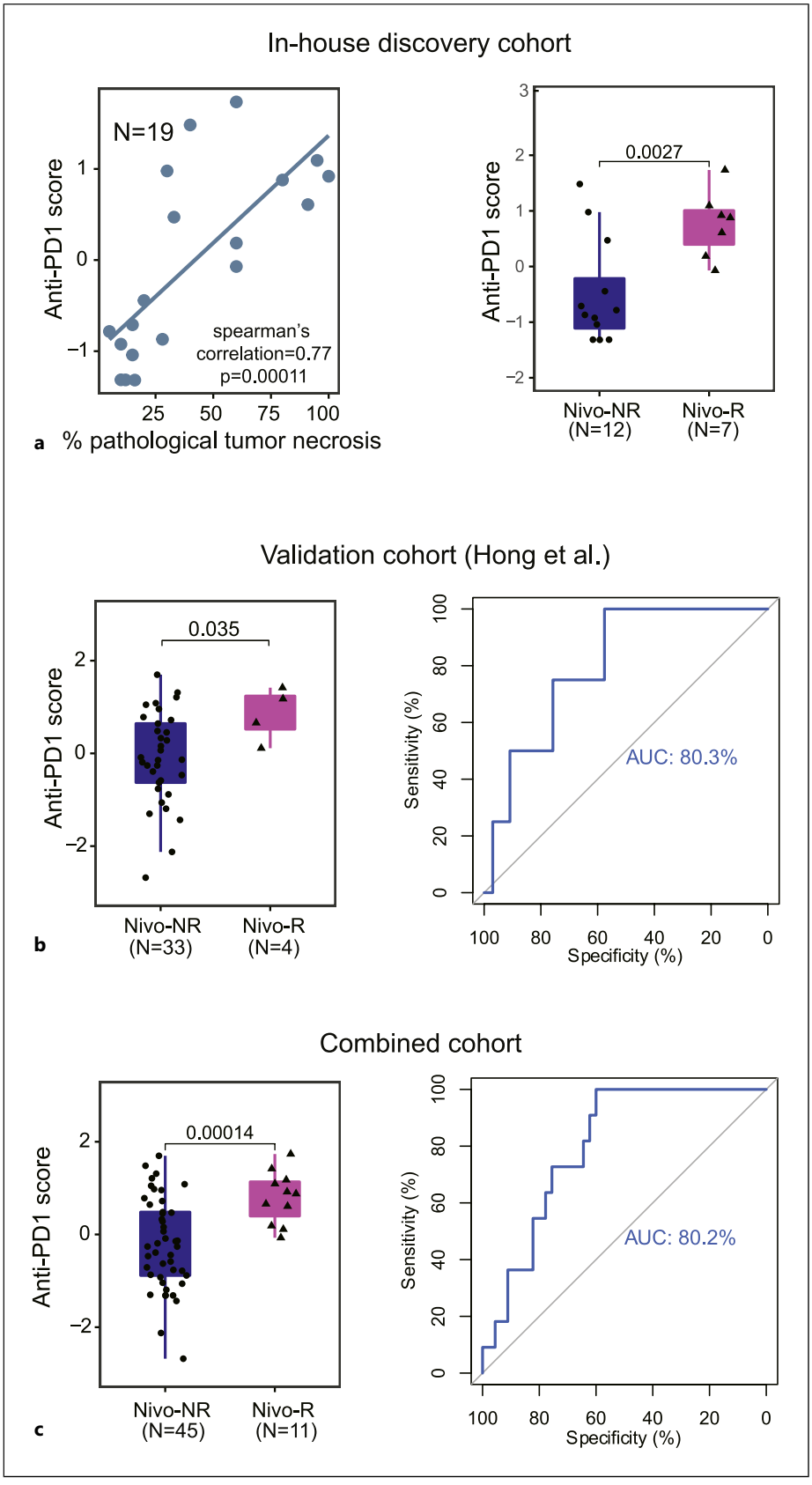

Fig. 7. CNV-based anti-PD-1 score predicted patients' response toward anti-PD-1 blockade. **a** Anti-PD-1 score associated with tumor necrosis outcome in nivolumab-treated patients (left panel). Nivolumab responsive and nonresponsive patients differed in terms of anti-PD-1 score using in-house sample cohort (2-sided *t* test, right panel). **b** Validation of anti-PD-1 score in determining anti-PD-1 blockade response using a Korean patient sample cohort by Hong et al. **c** ROC analysis of using anti-PD-1 score as biomarker to predict treatment outcome using combined sample cohort (in-house cohort and Korean cohort by Hong et al.).

cell types upon nivolumab treatment between nivo-R and nivo-NR cases. There was a greater proportion of cases with increased CD8 T-cell infiltration after nivolumab treatment in the nivo-R group than in the nivo-NR group. This change in CD8 T cells was confirmed with IHC, and the IHC findings were consistent with those using immune deconvolution. This is in line with the finding from Ho et al. [35], whose study also identified higher CD8 T-cell infiltration in posttreatment surgical samples in patients responsive to combined treatment of cabozantinib and nivolumab than nonresponsive patients. With PD-1 inhibition by nivolumab to reactivate the CD8 T cells, it is expected that the increased CD8 T-cell infiltration will confer positive responsiveness of the HCC tumor toward the drug. On the other hand, our study found a trend of decreased CD4 memory resting T cells after nivolumab treatment in nivo-R but not nivo-NR patients. There was a relative shift from resting to activated CD4 memory T cells in the responsive cases, but a trend of reversed shift from activated to resting CD4 memory T cells in the nonresponsive cases. In a previous study, both CD4 memory resting and activated T cells were found to be associated with HCC patients with poorer prognosis [38]. As memory CD4 T cells typically represent the T-cell subsets produced during a primary immunogenic challenge and are persistent to generate a recall response to secondary challenge [39], whether the shift between the two activation statuses of CD4 memory T cells determines the physiologic responsiveness to nivolumab of HCC needs further investigation.

Although ICIs are thought to act through blocking the immune checkpoints, the treatment response with ICI may not be solely related to the level of the immune checkpoint proteins. A recent study has shown that although higher PD-L1 score was associated with more complete/partial response, complete response was also seen in PD-L1-negative patients [40]. It is likely that there are fundamental factors that determine the effectiveness of ICB as well as potential additional layers of bypass mechanism upon ICB. For instance, we found a significant increase in CTLA4 expression after nivolumab in all cases, suggesting a potential alternative immune escape mechanism elicited by HCC tumors. Intriguingly, there was also a general upregulation of other co-inhibitory checkpoint molecules in the nivo-R cases. Additionally, by comparing the transcriptomic profiles of the nivo-R and nivo-NR liver tumor biopsies (pre-nivolumab), we identified significant overexpression of the gene signature that governs innate immunity. The elevated antigen presentation elicited by innate immunity may provide a favorable immunogenic environment to support the action of ICB. In line with our findings, there have been clinical trials testing the combined administration of agonist for innate immunity (e.g., cGAS-STING agonists, phagocytosis check point blockade) and ICB [41–43]. Moreover, our finding on decreased resting mast cell proportion is in accordance with a recent study demonstrating the association of tumor-infiltrating mast cells with anti-PD-1 resistance in a humanized mouse melanoma model and implicating mast cell depletion for improving the efficacy of anti-PD-1 therapy [44].

In this study, we derived a CNV-based anti-PD-1 score using target-panel sequencing of cfDNA isolated from plasma samples collected before nivolumab treatment. This noninvasive CNV-based anti-PD-1 score in our discovery cohort was found to robustly predict the response of anti-PD-1 ICB. We relied on the tissue-derived data from an independent Korean cohort in the Hong et al. [6] study, as there is a lack of relevant publicly available cfDNA data. Taken altogether, these findings suggest the potential use of noninvasive blood-based biomarker to advise nivolumab treatment response. Further large-scale studies along these directions are awaited.

Despite our findings that might favor the neoadjuvant use of nivolumab in HCC patients and reveal the cellular and molecular basis of nivolumab response, there were limitations of this study. With this being a pilot study, the sample size of the patients was relatively small, and a larger sample cohort is needed for further investigation. The study had no control arm and a relatively short follow-up period of the patients. However, this study focused on the pathologic response and immune microenvironment analysis, and we could not obtain the appropriate tissue samples from historical cohort control arm for analysis. We aim to perform the clinical comparison in another study. Furthermore, it would be useful to evaluate the neoadjuvant use of drug combo or other second-line drugs.

Taken together, our study demonstrates that use of nivolumab is safe and effective in the neoadjuvant setting for intermediate and locally advanced HCCs. Significant immune cell-related tumor necrosis observed in the post-nivolumab hepatectomy specimens signifies that successful restoration of cytotoxic immunity is the key determinant for ICB response. More importantly, a short course of neoadjuvant therapy may deliver durable therapeutic outcome in a small subset of patients. In addition, noninvasive cfDNA biomarker could potentially predict anti-PD-1 ICB response.

Acknowledgments

The authors thank the Centre for PanorOmic Sciences Imaging at the LKS Faculty of Medicine of the University of Hong Kong for the facilities for sequencing and technical support. We also thank Mr. Martin Kai-Yeung Leung and Ms. Vikki Tang for technical assistance.

Statement of Ethics

Written informed consent was obtained from participants prior to the study. This study protocol was reviewed and approved by the Institutional Review Board of the University of Hong Kong/Hospital Authority Hong Kong West Cluster, approval numbers UW 17-056 and UW19-667.

Conflict of Interest Statement

TC Yau has a consulting or advisory role for and receives honoraria from Bristol Myers Squibb, MSD, Exelixis, Ipsen, Eisai, AstraZeneca, Bayer, Novartis, EMD Serono, AbbVie, Pfizer, Eli Lilly, Sirtex, SillaJen, Taiho, OrigiMed, New B Innovation, Sirtex, and H3 Biomedicine.

Funding Sources

The study was supported by the Hong Kong Research Grants Council (RGC) Theme-based Research Scheme (T12-704/16-R and T12-716/22-R), Innovation and Technology Commission grant to State Key Laboratory of Liver Research, University Development Fund of the University of Hong Kong, and Loke Yew Endowed Professorship award. Nivolumab was sponsored by Bristol Myers Squibb (Investigators Initiated Study, CA209-7KU). I.O.L. Ng is Loke Yew Professor in Pathology.

Author Contributions

Tan-To Cheung, Thomas Chung-Cheung Yau, and Irene Oi-Lin Ng provided the study concept and design. Tan-To Cheung, Daniel Wai-Hung Ho, Shirley Xueying Lyu, Qingyang Zhang, Yu-Man Tsui, and Irene Oi-Lin Ng interpreted and analyzed the data. Tan-To Cheung, Simon Hing-Yin Tsang, and Wong-Hoi She performed the surgery. Vince Wing-hang Lau and Edward Yin-Lun Chu provided liver biopsy support. Roland Ching-Yu Leung and Thomas Chung-Cheung Yau administered the drug to patients. Daniel Wai-Hung Ho, Yu-Man Tsui, and Irene Oi-Lin Ng performed the experiments. Joyce Man-Fong Lee, Tiffany Ching-Yun Yu, and Karen Man-Fong Sze collected the samples. Tan-To Cheung and Irene Oi-Lin Ng provided financial support and supervised the project. Tan-To Cheung, Daniel Wai-Hung Ho, and Irene Oi-Lin Ng wrote the manuscript. All authors approved the final version of the manuscript.

Data Availability Statement

Data are not publicly available due to ethical reasons. Further inquiries can be directed to the corresponding author.

References

1 Llovet JM, Kelley RK, Villanueva A, Singal AG, Pikarsky E, Roayaie S, et al. Hepatocellular carcinoma. Nat Rev Dis Primers. 2021;7(1):6.
2 El-Khoueiry AB, Sangro B, Yau T, Crocenzi TS, Kudo M, Hsu C, et al. Nivolumab in patients with advanced hepatocellular carcinoma (CheckMate 040): an open-label, non-comparative, phase 1/2 dose escalation and expansion trial. Lancet. 2017;389(10088):2492–502.
3 Yau T, Park JW, Finn RS, Cheng AL, Mathurin P, Edeline J, et al. Nivolumab versus sorafenib in advanced hepatocellular carcinoma (CheckMate 459): a randomised, multicentre, open-label, phase 3 trial. Lancet Oncol. 2022;23(1):77–90.
4 Finn RS, Qin S, Ikeda M, Galle PR, Ducreux M, Kim TY, et al. Atezolizumab plus bevacizumab in unresectable hepatocellular carcinoma. N Engl J Med. 2020;382(20):1894–905.
5 Haber PK, Castet F, Torres-Martin M, Andreu-Oller C, Puigvehí M, Miho M, et al. Molecular markers of response to anti-PD1 therapy in advanced hepatocellular carcinoma. Gastroenterology. 2023;164(1):72–88 e18.
6 Hong JY, Cho HJ, Sa JK, Liu X, Ha SY, Lee T, et al. Hepatocellular carcinoma patients with high circulating cytotoxic T cells and intratumoral immune signature benefit from pembrolizumab: results from a single-arm phase 2 trial. Genome Med. 2022;14(1):1.
7 Gordan JD, Kennedy EB, Abou-Alfa GK, Beg MS, Brower ST, Gade TP, et al. Systemic therapy for advanced hepatocellular carcinoma: ASCO guideline. J Clin Oncol. 2020;38(36):4317–45.
8 Bruix J, Chan SL, Galle PR, Rimassa L, Sangro B. Systemic treatment of hepatocellular carcinoma: an EASL position paper. J Hepatol. 2021;75(4):960–74.
9 Yau T, Tang VYF, Yao TJ, Fan ST, Lo CM, Poon RTP. Development of Hong Kong Liver Cancer staging system with treatment stratification for patients with hepatocellular carcinoma. Gastroenterology. 2014;146(7):1691–700.e3.
10 Chan LK, Ho DWH, Kam CS, Chiu EYT, Lo ILO, Yau DTW, et al. RSK2-inactivating mutations potentiate MAPK signaling and support cholesterol metabolism in hepatocellular carcinoma. J Hepatol. 2021;74(2):360–71.
11 Ma W, Ho DWH, Sze KMF, Tsui YM, Chan LK, Lee JMF, et al. APOBEC3B promotes hepatocarcinogenesis and metastasis through novel deaminase-independent activity. Mol Carcinog. 2019;58(5):643–53.
12 Husain A, Chiu YT, Sze KMF, Ho DWH, Tsui YM, Suarez EMS, et al. Ephrin-A3/EphA2 axis regulates cellular metabolic plasticity to enhance cancer stemness in hypoxic hepatocellular carcinoma. J Hepatol. 2022;77(2):383–96.
13 Ho DWH, Chan LK, Chiu YT, Xu IMJ, Poon RTP, Cheung TT, et al. TSC1/2 mutations define a molecular subset of HCC with aggressive behaviour and treatment implication. Gut. 2017;66(8):1496–506.
14 Liao Y, Smyth GK, Shi W. The R package Rsubread is easier, faster, cheaper and better for alignment and quantification of RNA sequencing reads. Nucleic Acids Res. 2019;47(8):e47.
15 Love MI, Huber W, Anders S. Moderated estimation of fold change and dispersion for RNA-seq data with DESeq2. Genome Biol. 2014;15(12):550.

16 Li B, Dewey CN. RSEM: accurate transcript quantification from RNA-Seq data with or without a reference genome. BMC Bioinformatics. 2011;12:323.
17 Newman AM, Steen CB, Liu CL, Gentles AJ, Chaudhuri AA, Scherer F, et al. Determining cell type abundance and expression from bulk tissues with digital cytometry. Nat Biotechnol. 2019;37(7):773–82.
18 Chen J, Bardes EE, Aronow BJ, Jegga AG. ToppGene Suite for gene list enrichment analysis and candidate gene prioritization. Nucleic Acids Res. 2009;37(Web Server issue):W305–11.
19 Szklarczyk D, Gable AL, Nastou KC, Lyon D, Kirsch R, Pyysalo S, et al. The STRING database in 2021: customizable protein-protein networks, and functional characterization of user-uploaded gene/measurement sets. Nucleic Acids Res. 2021;49(D1):D605–12.
20 Talevich E, Shain AH, Botton T, Bastian BC. CNVkit: genome-wide copy number detection and visualization from targeted DNA sequencing. PLoS Comput Biol. 2016;12(4):e1004873.
21 Musunuri R, Arora K, Corvelo A, Shah M, Shelton J, Zody MC, et al. Somatic variant analysis of linked-reads sequencing data with Lancet. Bioinformatics. 2021;37(13):1918–9.
22 Cibulskis K, Lawrence MS, Carter SL, Sivachenko A, Jaffe D, Sougnez C, et al. Sensitive detection of somatic point mutations in impure and heterogeneous cancer samples. Nat Biotechnol. 2013;31(3):213–9.
23 Mouliere F, Chandrananda D, Piskorz AM, Moore EK, Morris J, Ahlborn LB, et al. Enhanced detection of circulating tumor DNA by fragment size analysis. Sci Transl Med. 2018;10(466):eaat4921.
24 Ho DW, Sze KM, Ng IO. Virus-Clip: a fast and memory-efficient viral integration site detection tool at single-base resolution with annotation capability. Oncotarget. 2015;6(25):20959–63.
25 Wai-Hung Ho D, Lyu X, Oi-Lin Ng I. Viral integration detection strategies and a technical update on Virus-Clip. Biocell. 2021;45(6):1495–500.
26 Jin H, Liu Z. A benchmark for RNA-seq deconvolution analysis under dynamic testing environments. Genome Biol. 2021;22(1):102.
27 Avila Cobos F, Alquicira-Hernandez J, Powell JE, Mestdagh P, De Preter K. Benchmarking of cell type deconvolution pipelines for transcriptomics data. Nat Commun. 2020;11(1):5650.
28 McGrail DJ, Pilié PG, Rashid NU, Voorwerk L, Slagter M, Kok M, et al. High tumor mutation burden fails to predict immune checkpoint blockade response across all cancer types. Ann Oncol. 2021;32(5):661–72.
29 Sangro B, Sarobe P, Hervás-Stubbs S, Melero I. Advances in immunotherapy for hepatocellular carcinoma. Nat Rev Gastroenterol Hepatol. 2021;18(8):525–43.
30 Horn S, Leonardelli S, Sucker A, Schadendorf D, Griewank KG, Paschen A. Tumor cdkn2a-associated JAK2 loss and susceptibility to immunotherapy resistance. J Natl Cancer Inst. 2018;110(6):677–81.
31 Adib E, Nassar AH, Akl EW, Abou Alaiwi S, Nuzzo PV, Mouhieddine TH, et al. CDKN2A alterations and response to immunotherapy in solid tumors. Clin Cancer Res. 2021;27(14):4025–35.
32 Yau T, Hsu C, Kim TY, Choo SP, Kang YK, Hou MM, et al. Nivolumab in advanced hepatocellular carcinoma: sorafenib-experienced Asian cohort analysis. J Hepatol. 2019;71(3):543–52.
33 Yau T, Kang YK, Kim TY, El-Khoueiry AB, Santoro A, Sangro B, et al. Efficacy and safety of nivolumab plus ipilimumab in patients with advanced hepatocellular carcinoma previously treated with sorafenib: the CheckMate 040 randomized clinical trial. JAMA Oncol. 2020;6(11):e204564.
34 Simoes CC, Thung SN, Fiel MI, Sung MW, Schwartz ME, Ward SC. Morphology of tumor and nontumor tissue in liver resection specimens for hepatocellular carcinoma following nivolumab therapy. Mod Pathol. 2021;34(4):823–33.
35 Ho WJ, Zhu Q, Durham J, Popovic A, Xavier S, Leatherman J, et al. Neoadjuvant cabozantinib and nivolumab converts locally advanced HCC into resectable disease with enhanced antitumor immunity. Nat Cancer. 2021;2(9):891–903.
36 Marron TU, Fiel MI, Hamon P, Fiaschi N, Kim E, Ward SC, et al. Neoadjuvant cemiplimab for resectable hepatocellular carcinoma: a single-arm, open-label, phase 2 trial. Lancet Gastroenterol Hepatol. 2022;7(3):219–29.
37 Kaseb AO, Hasanov E, Cao HST, Xiao L, Vauthey JN, Lee SS, et al. Perioperative nivolumab monotherapy versus nivolumab plus ipilimumab in resectable hepatocellular carcinoma: a randomised, open-label, phase 2 trial. Lancet Gastroenterol Hepatol. 2022;7(3):208–18.
38 Kong J, Yu G, Si W, Li G, Chai J, Liu Y, et al. Identification of a glycolysis-related gene signature for predicting prognosis in patients with hepatocellular carcinoma. BMC Cancer. 2022;22(1):142.
39 Gasper DJ, Tejera MM, Suresh M. CD4 T-cell memory generation and maintenance. Crit Rev Immunol. 2014;34(2):121–46.
40 Sangro B, Melero I, Wadhawan S, Finn RS, Abou-Alfa GK, Cheng AL, et al. Association of inflammatory biomarkers with clinical outcomes in nivolumab-treated patients with advanced hepatocellular carcinoma. J Hepatol. 2020;73(6):1460–9.
41 Wang Y, Luo J, Alu A, Han X, Wei Y, Wei X. cGAS-STING pathway in cancer biotherapy. Mol Cancer. 2020;19(1):136.
42 Feng M, Jiang W, Kim BYS, Zhang CC, Fu YX, Weissman IL. Phagocytosis checkpoints as new targets for cancer immunotherapy. Nat Rev Cancer. 2019;19(10):568–86.
43 Rothlin CV, Ghosh S. Lifting the innate immune barriers to antitumor immunity. J Immunother Cancer. 2020;8(1):e000695.
44 Somasundaram R, Connelly T, Choi R, Choi H, Samarkina A, Li L, et al. Tumor-infiltrating mast cells are associated with resistance to anti-PD-1 therapy. Nat Commun. 2021;12(1):346.